

---

---

ELECTRICAL AND MAGNETIC  
PROPERTIES

---

---

## Neutron Diffraction Study of the Effect of Changes in the Crystal Structure of $A_2MnTeO_6$ ( $A = Ag, Tl$ ) on the Spin Configuration

A. E. Susloparova<sup>a, \*</sup> and A. I. Kurbakov<sup>a</sup>

<sup>a</sup> *St. Petersburg Institute of Nuclear Physics, National Research Center Kurchatov Institute, Orlova roshcha, Gatchina, Leningradskaya oblast, 188300 Russia*

*\*e-mail: susloparova\_ae@npni.nrcki.ru*

Received November 17, 2021; revised January 31, 2022; accepted February 20, 2022

**Abstract**—The neutron diffraction studies of powder samples from the family of  $A_2MnTeO_6$  tellurates ( $A = Ag, Tl$ ) were performed at room and low temperatures. The specific features of their crystal structure were investigated, and the partial substitution of Mn and Te atoms was revealed. The spin structure of  $Ag_2MnTeO_6$  was determined in an ordered state at  $T = 1.6$  K by symmetry and full-profile analysis. It represented a non-collinear  $120^\circ$  triangular structure in the  $ab$  plane and a spin helicoid along the  $c$ -axis with the propagation vector  $\mathbf{k} = (1/3\ 1/3\ 1/3)$ . The neutron diffraction measurements of  $Tl_2MnTeO_6$  did not reveal any additional reflections associated with the organization of long-range magnetic order up to  $T = 1.6$  K. The studied compounds were compared with the powders belonging to the same family and the earlier published results, which served to reveal a similarity between their crystal and magnetic structures and  $Na_2MnTeO_6$  and a radically different type of their magnetic ordering as compared to  $Li_2MnTeO_6$ .

**Keywords:** low-dimensional magnetism, neutron powder diffraction, frustration of exchange interactions

**DOI:** 10.1134/S0031918X22070171

### INTRODUCTION

$Ag_2MnTeO_6$  and  $Tl_2MnTeO_6$  studied here belong to the new structural family  $A_2MnTeO_6$ , where  $A$  is a monovalent ion. The information about this family of tellurates was published for the first time in [1]. In the mentioned paper, most attention was focused on the methods for the synthesis of samples and their standard characterization from the viewpoint of their crystal structure and micromagnetic properties. Afterwards, more detailed studies were performed for  $Li_2MnTeO_6$  [2] and  $Na_2MnTeO_6$  [3], where unusual magnetic properties were revealed, and some models describing the magnetic state at low temperatures were proposed. All the compounds of  $A_2MnTeO_6$  are characterized by the arrangement of magnetic ions in triangular geometry, which provides the conditions for the appearance of frustration of exchange interactions in the magnetic subsystem in combination with a layered structure. Low-dimensional magnets manifest the quantum nature most clearly when magnetic interactions begin to dominate over temperature fluctuations, and it becomes possible to observe a set of quantum cooperative effects. The effect of anisotropy and frustration in such systems essentially grows, and the attainment of long-range magnetic order becomes strongly hindered.

This paper represents the studies of specific features of the crystal structure and spin state of  $Ag_2MnTeO_6$  and

$Tl_2MnTeO_6$  and the comparison of results with earlier published data for  $Li_2MnTeO_6$  and  $Na_2MnTeO_6$ . We revealed not only some similarities between the structures, but also serious distinctions between their magnetic subsystems which can be explained by the change in the interlayer distance.

### EXPERIMENTAL

A polycrystalline  $Na_2MnTeO_6$  sample was prepared by solid-state synthesis, mixing with the corresponding oxides with further prolonged baking, and the technology and conditions of synthesis are detailed in [1].  $Ag_2MnTeO_6$  and  $Tl_2MnTeO_6$  investigated in that study were synthesized by the ion-exchange reaction from  $Na_2MnTeO_6$  prepared by direct synthesis. The reasons, for which the direct synthesis of compositions  $Ag$  and  $Tl$  is unfeasible, are explained in detail in [1].

The morphological analysis of powders was performed by scanning electron microscopy (SEM) in the European Synchrotron Radiation Facility (ESRF) Center (Grenoble, France).

Neutron diffraction studies were carried out on the SINQ source of neutrons in the Paul Scherrer Institute (Switzerland) with the use of two different powder diffractometers with thermal (HRPT) and cold (DMC) neutrons. The crystal structure parameters were

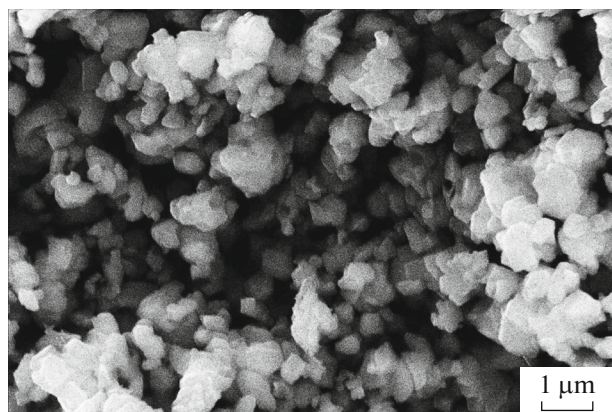


Fig. 1. SEM photo of  $\text{Tl}_2\text{MnTeO}_6$ .

refined using the data of experiments at room temperature, whereas magnetic scattering was detected at a temperature of 1.6 K. When the HRPT diffractometer was used, monochromatic neutrons with a wavelength of 1.886 Å were obtained by means of single-crystal germanium monochromator reflection ( $hkk$ ) = (511) in a high intensity (HI) mode. The fixed monochromator angle of  $2\theta_M$  used to perform scanning with a step of  $0.05^\circ$  within a range of diffraction angles of  $3.55^\circ$ – $164.50^\circ$  was  $120^\circ$ . In the process of measurement, the samples were placed into a thin-wall cylindrical vanadium container of  $6 \times 50$  mm in size.

### CRYSTAL STRUCTURE SPECIFIC FEATURES

The specific features of the surface morphology of powder particles were studied on a scanning electron microscope. The grains have distinct boundaries and an average size of 1 μm (Fig. 1).

The measured experimental neutron diffraction patterns were processed by the full-profile Rietveld analysis method in the FullProf software suite [4]. The analysis results were used to construct the models of unit cells for these compounds by the VESTA data visualization software [5] for two temperatures of 1.6 and 300 K, at which measurements were carried out.

Neutron powder diffraction experiments were conducted within a broad range of temperatures from helium to room temperature. The quality of processing the experimental data measured on a high-resolution HRPT diffractometer at room temperature by the Rietveld method is illustrated in Fig. 2.

The crystal structure of these samples, into which all the samples from the  $\text{A}_2\text{MnTeO}_6$  family crystallize, was earlier interpreted by laboratory X-ray diffraction as belonging space group  $P\text{-}31c$  [1]. As a result of processing the neutron diffraction data, we not only confirmed the proposed model and refined the characteristics of some of its fragments, but also revealed the displacement of Mn and Te ions due to a considerable

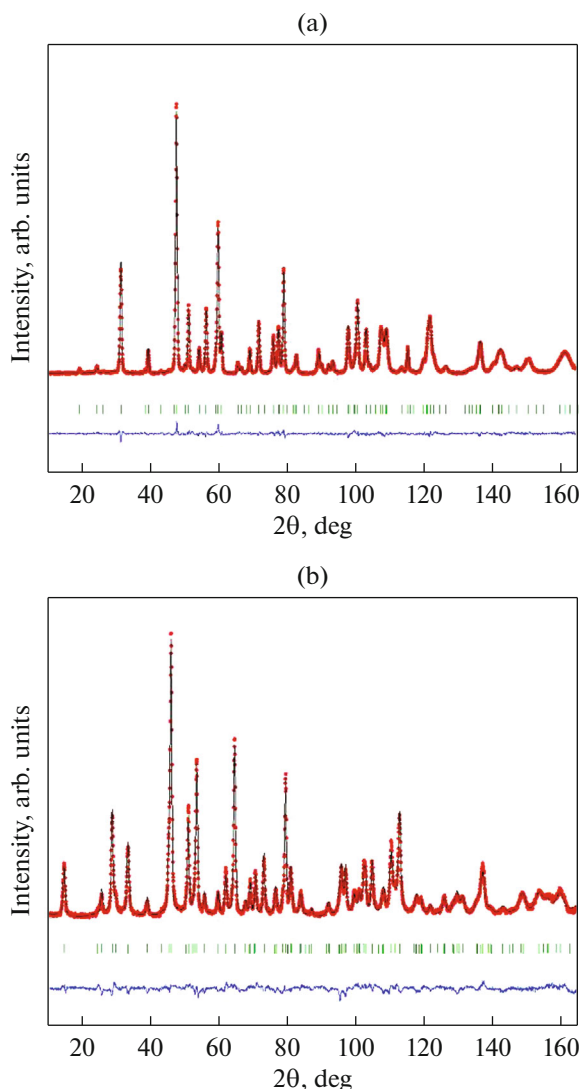
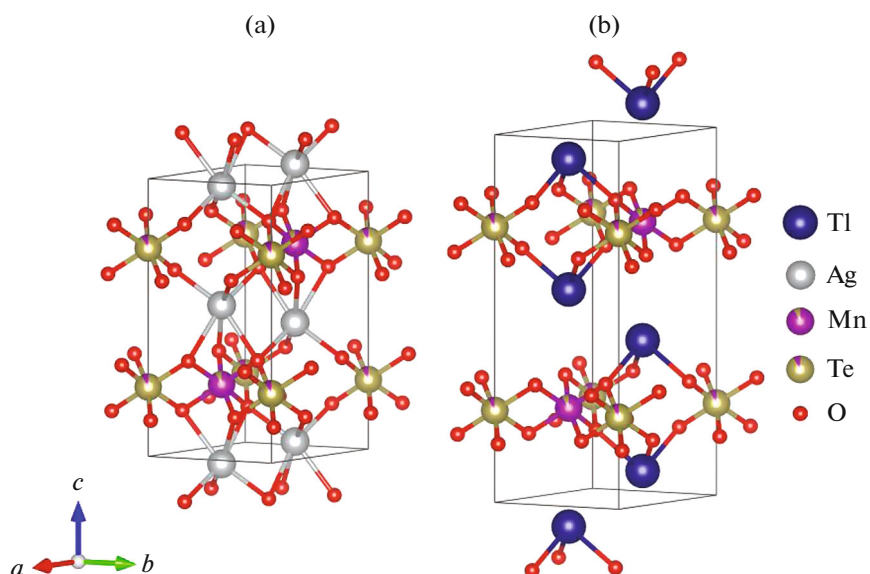


Fig. 2. Full-profile analysis of neutron diffraction data measured for (a)  $\text{Ag}_2\text{MnTeO}_6$  and (b)  $\text{Tl}_2\text{MnTeO}_6$  at room temperature: experimental data (red points), calculated profile (black line), difference between the experimental and calculated data (blue line), and positions of Bragg reflections (green vertical strokes).

difference between the values and even signs of neutron scattering length for Mn ( $-3.73$  fm) and Te (5.80 fm).

The crystal structure represents honeycomb (hexagonal) layers of  $\text{Mn}^{4+}$  and  $\text{Te}^{6+}$  cations, which are alternated along the  $c$ -axis with nonmagnetic layers composed of  $\text{Ag}^+$  or  $\text{Tl}^+$ . All the ions are located inside octahedra the vertices of which are oxygen anions (Fig. 3). However, there also are some distinctions. The compound with the  $\text{Tl}^+$  ion differs from the three others compounds of the tellurate family. In  $\text{Tl}_2\text{MnTeO}_6$ , thallium has an actual coordination number of 3 instead of 6, which results in the separation of a layer. This is associated with the effect of an unshared electron pair, which was discussed in more detail in [1].



**Fig. 3.** Refined models of the crystal structure of  $A_2MnTeO_6$  ( $A = Ag, Tl$ ). Different colors within the same sphere correspond to 8% Mn/Te structural substitution.

The used crystal structure model describes all of the diffraction peaks and no impurities have been revealed. As a result, we acquired highly precise information on the structural parameters, such as the positions of all the atoms in the unit cell, the occupation of atomic positions, the thermal factors, bond lengths, and bond angles, which influence the magnetic properties of the studied materials; the principal characteristics are compiled in Table 1.

The complexes of Mn and Te cations are organized as a honeycomb configuration. Here, the subsystem of manganese ions forms a triangular lattice, and the frustration of magnetic interactions should be expected in the case of antiferromagnetic type of interaction between manganese ions at a low temperature.

The compounds of the  $A_2MnTeO_6$  family ( $A = Li, Na, Ag, Tl$ ) have a similar crystal structure. However, an increase in the ionic radii from  $Li^+$  to  $Na^+$ ,  $Ag^+$ , and  $Tl^+$  leads to a monotonic increase in the interlayer spacing; unit cell parameter  $c$  changes by 54%, while parameter  $a$  changes nonmonotonically by only 2.3%. The parameters are compared in Table 2.

### MAGNETIC STRUCTURE

The neutron diffraction pattern, which was recorded on HRPT for  $Ag_2MnTeO_6$  at  $T = 1.6$  K and demonstrate the appearance of additional Bragg reflections as compared to the neutron diffraction pattern measured at room temperature, is shown in Fig. 4.

**Table 1.** Unit cell characteristics for  $Ag_2MnTeO_6$  and  $Tl_2MnTeO_6$ : position, coordinates, and occupation

Atom	Position	$x$	$Y$	$z$	Occupation
$Ag_2MnTeO_6$					
Ag	4f	2/3	1/3	0.9644(1)	0.333
Mn	2d	2/3	1/3	1/4	0.153(1)
Te	2a	0	0	1/4	0.153
O	12i	0.0512(1)	0.7143(1)	0.6530(3)	1
$Tl_2MnTeO_6$					
Tl	4f	2/3	1/3	0.9279(2)	0.333
Mn	2d	2/3	1/3	1/4	0.155(1)
Te	2a	0	0	1/4	0.155
O	12i	0.0436(1)	0.7064(1)	0.6773 (3)	1

**Table 2.** Unit cell parameters determined for  $A_2MnTeO_6$  ( $P-31c$ ) from neutron diffraction data

	$Li_2MnTeO_6$	$Na_2MnTeO_6$	$Ag_2MnTeO_6$	$Tl_2MnTeO_6$
$a = b$	5.01393(4)	5.11576(3)	5.13252(3)	5.11425(7)
$c$	9.5175(3)	10.5701(9)	11.1621(1)	14.6605(4)
$V$	207.210(1)	239.570(3)	254.646(3)	332.08(1)

In the inset to Fig. 4, new reflections can be clearly seen within the angular range from  $10^\circ$  to  $25^\circ$ . Judging by the appearance of magnetic peaks, at angles smaller than for the first nuclear reflection (002), it is possible to conclude that the long-range antiferromagnetic order is established at low temperatures. The phase transition from the paramagnetic to antiferromagnetic state with decreasing temperature is observed without any noticeable structural transformations.

In contrast to  $Ag_2MnTeO_6$ , the neutron diffraction pattern measured for  $Tl_2MnTeO_6$  also at  $T = 1.6$  K contains only the nuclear reflections from the crystal lattice, thus verifying that this compound has no long-range magnetic order up to 1.6 K.

The processing of the low-temperature neutron powder diffraction pattern of  $Ag_2MnTeO_6$  is given in Fig. 5. As a result of symmetry analysis performed for the positions of the most intense magnetic reflections by the BasIreps software (FULLPROF software suite), the propagation vector  $\mathbf{k} = (1/3 \ 1/3 \ 1/3)$  was found. This corresponds to a comparable spin structure, whose magnetic cell is tripled as compared to a crystal unit cell in all crystallographic directions.

The magnetic structure obtained for  $Ag_2MnTeO_6$  as a result of Rietveld analysis is shown in Fig. 6.

The magnetic ions located in the octahedral oxygen surrounding form a triangular structure within a layer. When passing from layer to layer in a magnetic unit cell, the magnetic moments at the manganese atoms in position  $(2/3 \ 1/3 \ 1/4)$  rotate at  $120^\circ$  in the clockwise direction (to the right), and at the atoms in position  $(1/3 \ 2/3 \ 1/4)$ , in the counterclockwise direction (to the left) in the  $ab$  plane (Fig. 6, lower inset).

The magnetic moments in each spin triangle are directed off the center of a triangle. There are six layers of manganese ions ordered in the form of a spin helicoid along the crystallographic direction  $c$  per magnetic unit cell. Such a structure is similar to the spin state of  $Na_2MnTeO_6$  and radically differs from  $Li_2MnTeO_6$ , whose magnetic unit cell is composed of two layers of Mn ions.

The magnetic moment of manganese ions in each magnetoactive  $MnTeO_6$  layer is  $1.18 \mu_B/Mn$  ( $m_x = 0.68(1) \mu_B/Mn$ ,  $m_y = 1.36(3) \mu_B/Mn$ ) for  $Ag_2MnTeO_6$ . At the same time, the magnetic moment of the similar  $Na_2MnTeO_6$  structure is  $1.8 \mu_B/Mn$ .

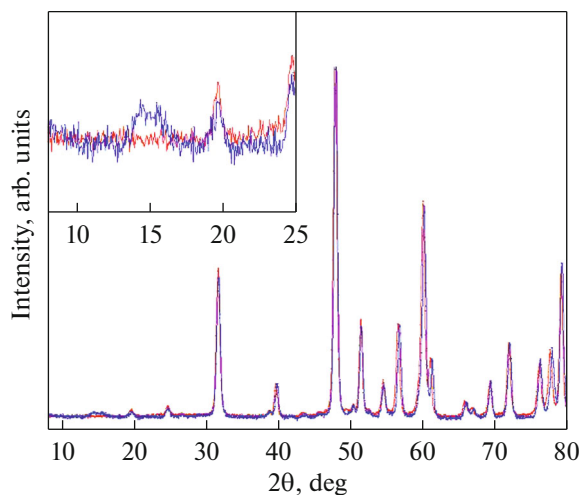


**Fig. 4.** Experimental neutron diffraction patterns measured for  $Ag_2MnTeO_6$  at temperatures of 1.6 (blue) and 300 K (red) with small-angle region (inset).

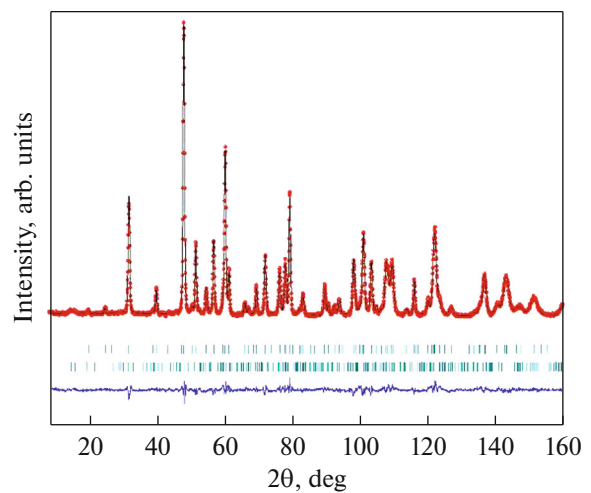


**Fig. 5.** Full-profile analysis of neutron diffraction data for  $Ag_2MnTeO_6$  at 1.6 K with positions of Bragg reflections (upper row of vertical strokes) and magnetic Bragg reflections (lower row of vertical strokes).

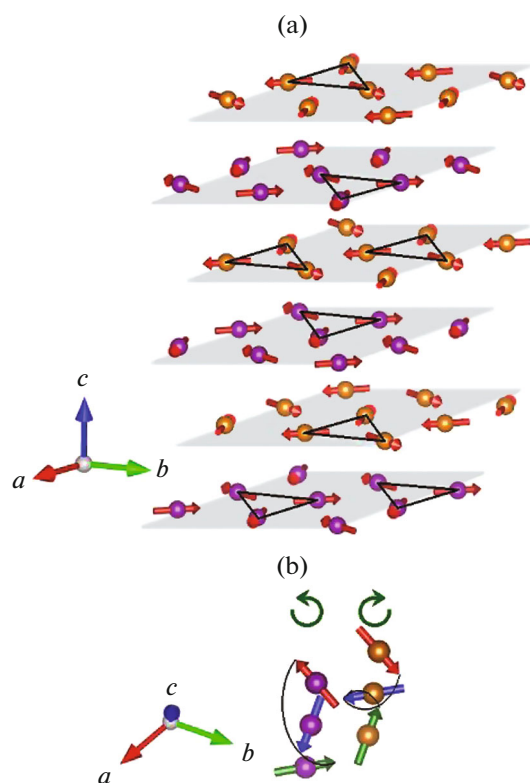


Fig. 6. Magnetic structure of  $\text{Ag}_2\text{MnTeO}_6$  at a temperature of 1.6 K.

Low values of magnetic moments for  $\text{Mn}^{4+}$ ,  $d^3$ ,  $S = 3/2$ , and ( $\mu_{\text{theor}} = 3.87 \mu_{\text{B}}$ ) indicate the incomplete formation of spin structure in  $\text{Ag}_2\text{MnTeO}_6$  at  $T = 1.6$  K.

Despite an identical structure of all representatives of this family, magnetic scattering detected on HRPT for  $\text{Ag}_2\text{MnTeO}_6$  is the same as for  $\text{Na}_2\text{MnTeO}_6$  and differs from  $\text{Li}_2\text{MnTeO}_6$ , which were studied earlier. The peaks produced by magnetic scattering from the compounds with Ag and Na have the same position in contrast to  $\text{Li}_2\text{MnTeO}_6$ , which indicates the existence of different propagation vectors. However, the intensity is different in all three cases, as well as the magnetic moment value, as clearly illustrated in Fig. 7.

We explain the decrease in the magnetic moment from the sodium to silver samples with the difference between parameters  $c$  of crystal unit cells ( $\approx 9.5$  Å and 14.7 Å, see Table 2). This results in a weaker interplanar exchange bonding and prevents the formation of three-dimensional magnetic order in the studied samples.

## CONCLUSIONS

The crystal structure of  $\text{Ag}_2\text{MnTeO}_6$  and  $\text{Tl}_2\text{MnTeO}_6$ , which belong to the family of layered  $\text{A}_2\text{MnTeO}_6$  tellurates ( $A = \text{Li}, \text{Na}, \text{Ag}, \text{Tl}$ ), has been confirmed and refined by high-resolution neutron powder diffraction. The samples crystallize into the structure with

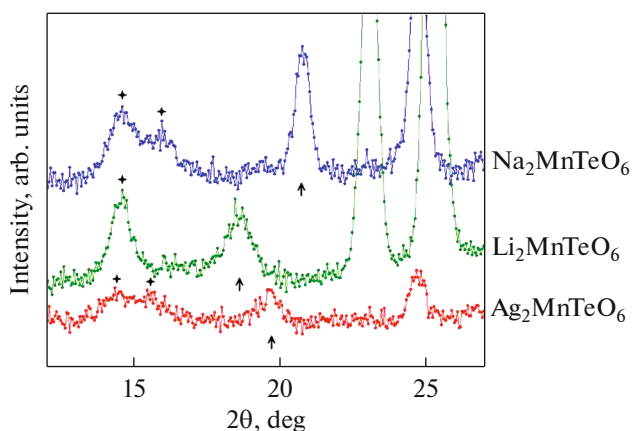


Fig. 7. Small-angle neutron diffraction data for  $\text{Ag}_2\text{MnTeO}_6$ ,  $\text{Li}_2\text{MnTeO}_6$ , and  $\text{Na}_2\text{MnTeO}_6$  at low temperature.

the space group  $P-31c$ , and represent alternating magnetoactive  $(\text{MnTeO}_6)^{2-}$  and nonmagnetic layers with a honeycomb structure.

It has been demonstrated that the unit cell parameter  $c$ , which characterizes the interlayer distances and depends on the radius of a monovalent  $A$  metal, has an essential effect on the magnetic properties. The magnetic structure of  $\text{Ag}_2\text{MnTeO}_6$  is similar to  $\text{Na}_2\text{MnTeO}_6$  [3] and radically differs from the compound containing lithium with a much smaller ionic radius.

The spin configuration in the ground state of  $\text{Ag}_2\text{MnTeO}_6$  has been determined by processing the neutron diffraction data measured at  $T = 1.6$  K. The magnetic structure model represents a comparable antiferromagnetic  $120^\circ$  triangular structure laying in the  $ab$  plane and a spin helicoil along the  $c$ -axis with the propagation vector  $\mathbf{k} = (1/3 \ 1/3 \ 1/3)$ .

$\text{Tl}_2\text{MnTeO}_6$  with the largest ionic radius of element  $A$  does not exhibit any additional neutron scattering due to the establishment of long-range magnetic order up to 1.6 K.

## ACKNOWLEDGMENTS

This study was performed on the Swiss SINQ source of neutrons at the Paul Scherrer Institute. The authors are grateful to V.B. Nalbandyan (Southern Federal University) for the synthesis of samples and V.Yu. Pomyakushin for help in experiments.

## FUNDING

This study was supported by the Russian Scientific Foundation (grant no. 18-12-00375, <https://rscf.ru/project/18-12-00375/>).

## REFERENCES

1. V. B. Nalbandyan, I. L. Shukaev, G. V. Raganyan, A. Svyazhin, A. N. Vasiliev, E. A. Zvereva, "Preparation, crystal chemistry, and hidden magnetic order in the family of trigonal layered tellurates  $A_2Mn^{(4+)}TeO_6$  ( $A = Li, Na, Ag, \text{ or } Tl$ )," *Inorg. Chem.* **58**, No. 9, 5524–5532 (2019).
2. E. A. Zvereva, G. V. Raganyan, T. M. Vasilchikova, V. B. Nalbandyan, D. A. Gafurov, E. L. Vavilova, K. V. Zakharov, H.-J. Koo, V. Yu. Pomjakushin, A. E. Susloparova, A. I. Kurbakov, A. N. Vasiliev, and M.-H. Whangbo, "Hidden magnetic order in the triangular-lattice magnet  $Li_2MnTeO_6$ ," *Phys. Rev. B* **102**, No. 9, 094433 (2020).
3. A. I. Kurbakov, A. E. Susloparova, V. Yu. Pomjakushin, Y. Skourski, G. V. Raganyan, T. M. Vasilchikova, E. L. Vavilova, and A. N. Vasiliev, "Magnetic order in triangular-lattice layered magnets  $Na_2MnTeO_6$ ," *Phys. Rev. B* **105**, No. 9, 064416 (2022).
4. FULLPROF suite, <http://www.ill.eu/sites/fullprof/>.
5. VESTA, Visualization for Electron and Structural Analysis, <https://jp-minerals.org/vesta/>.

*Translated by E. Glushachenkova*